

# Characteristics of Atmosphere-Skimming air showers relevant for high-altitude radio experiments

Sergio Cabana Freire<sup>a</sup>, Jaime Álvarez Muñiz<sup>a</sup> and Matías Tueros<sup>b</sup>

<sup>a</sup>Instituto Galego de Física de Altas Enerxías, Universidade de Santiago de Compostela

<sup>b</sup>Instituto de Física La Plata. CONICET - UNLP

June 12, 2024



CHICAGO 2024

- 1 Introduction & Motivation
- 2 Air shower development
- 3 Characteristics of the radio emission
- 4 Conclusion & Outlook

1 Introduction & Motivation

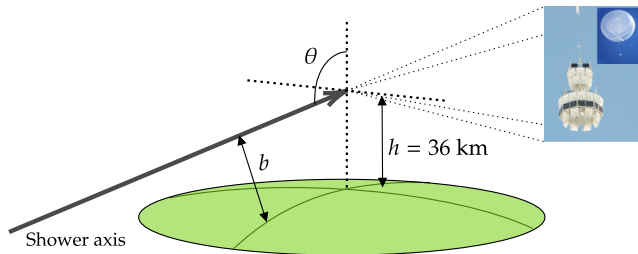
2 Air shower development

3 Characteristics of the radio emission

4 Conclusion & Outlook

# Introduction & Motivation

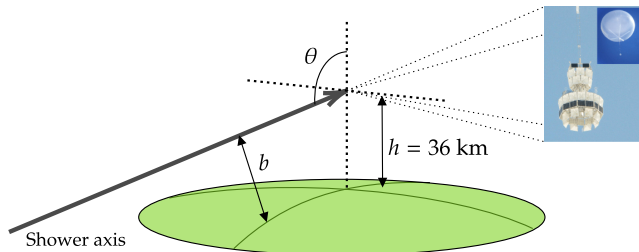
- Air showers developing in the atmosphere without intercepting ground



- Propagation across very low densities under the effect of the geomagnetic field

# Introduction & Motivation

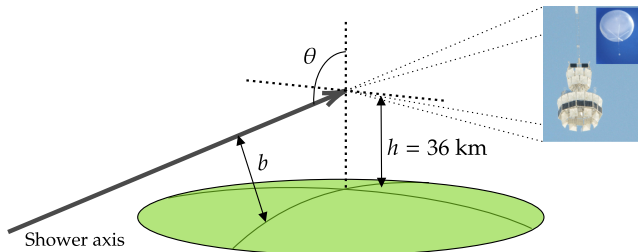
- Air showers developing in the atmosphere without intercepting ground



- Propagation across very low densities under the effect of the geomagnetic field
- 7 atmosphere-skimming events detected in ANITA flights. Recent observations by EUSO-SPB2

# Introduction & Motivation

- Air showers developing in the atmosphere without intercepting ground



- Propagation across very low densities under the effect of the geomagnetic field
- 7 atmosphere-skimming events detected in ANITA flights. Recent observations by EUSO-SPB2
- *RASPASS*: Version of ZHAireS allowing simulations of any geometry.

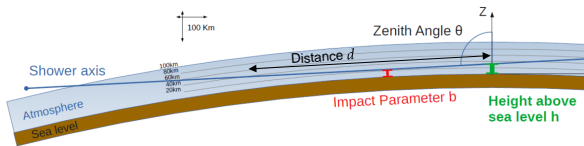
1 Introduction & Motivation

2 Air shower development

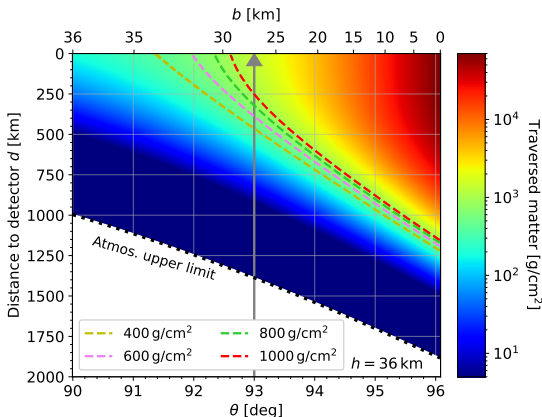
3 Characteristics of the radio emission

4 Conclusion & Outlook

# Parameter space for shower development



- Balloon-borne detector:  $h = 36$  km

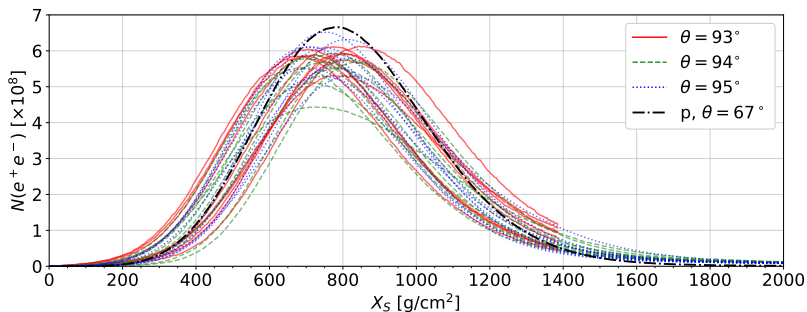


- Available matter for shower development and impact parameter restrict *detectable* geometries



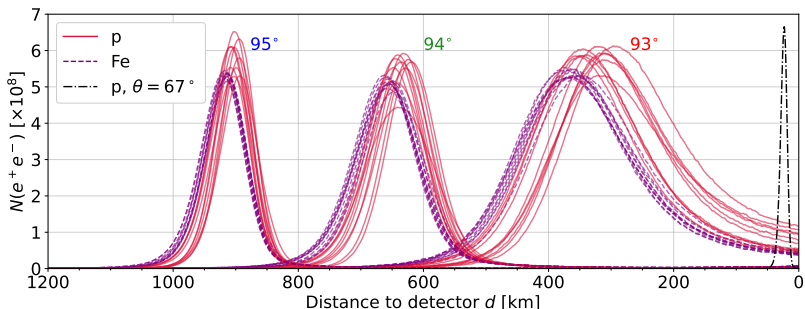
# Longitudinal development

- $\langle X_{\max} \rangle$  and  $\sigma(X_{\max})$  similar to downward-going showers in units of  $\text{g}/\text{cm}^2$



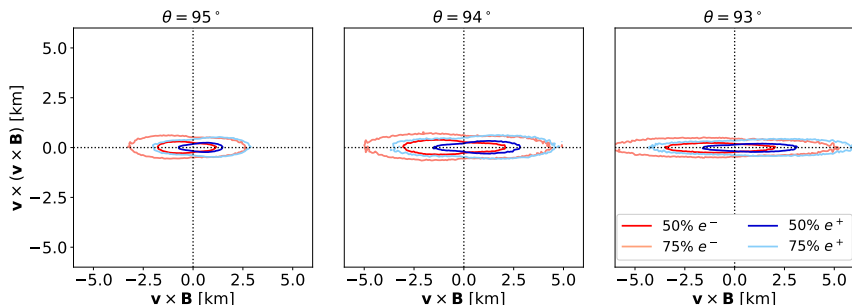
# Longitudinal development

- $\langle X_{\max} \rangle$  and  $\sigma(X_{\max})$  similar to downward-going showers in units of  $\text{g}/\text{cm}^2$
- Showers stretching distances of hundreds of km, increasing for cascades developing higher in the atmosphere
- Fluctuations in  $X_{\max}$  reach the order of tens km



# Lateral development at $X_{\max}$

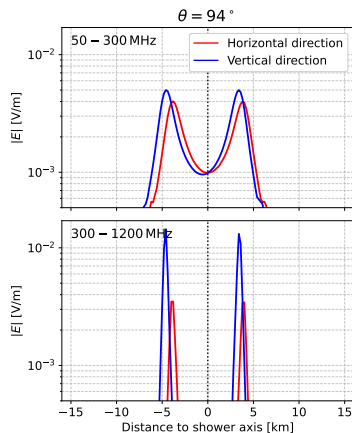
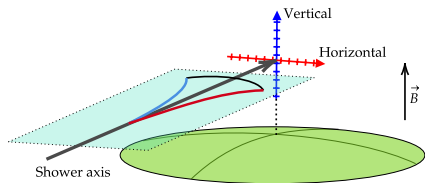
- Showers develop across huge distances under the geomagnetic field
- *Flattening* of the shower front in the  $\mathbf{v} \times \mathbf{B}$  direction
- Effect enhanced as cascades propagate in lower densities (smaller  $\theta$ )



- 1 Introduction & Motivation
- 2 Air shower development
- 3 Characteristics of the radio emission
- 4 Conclusion & Outlook

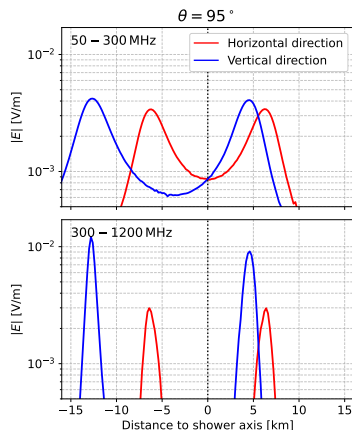
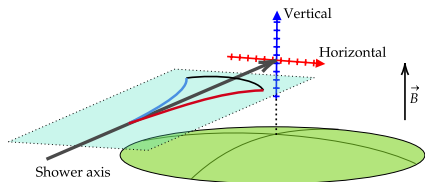
# Lateral distribution of the signal

- Geometry and dimensions of cascades affect their radio emission
- Radio LDF displaced downwards:  
*Refractive asymmetry*
- Enhanced for inclined showers.  
Independent of frequency



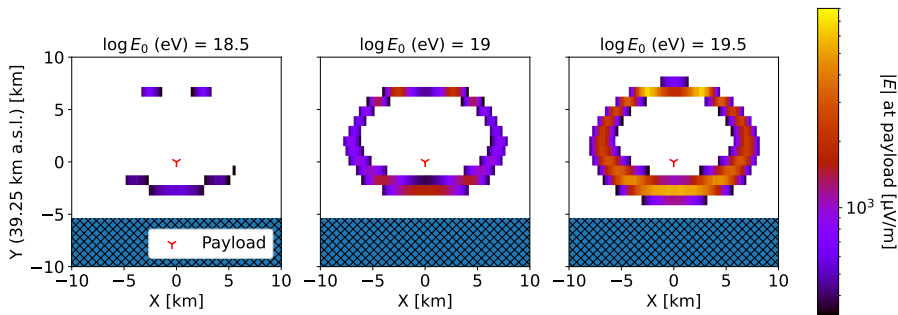
# Lateral distribution of the signal

- Geometry and dimensions of cascades affect their radio emission
- Radio LDF displaced downwards:  
*Refractive asymmetry*
- Enhanced for inclined showers. Independent of frequency



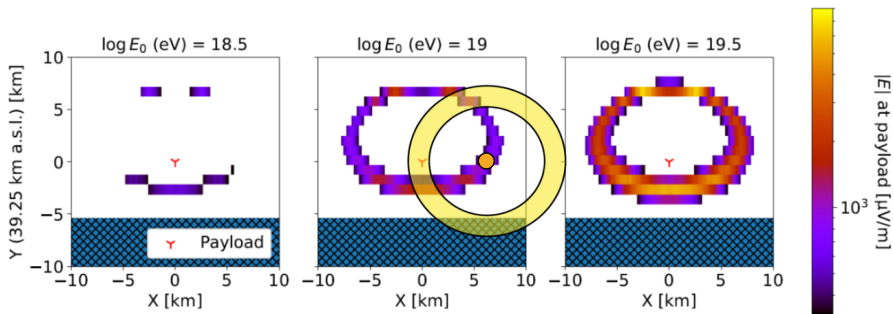
# Effects on aperture of balloon-borne experiments

- Asymmetries in the radio emission impact the effective area of high-altitude detectors
- Example: Showers producing signals above trigger threshold of ANITA, assuming elevation angle of event 9734523 of ANITA IV ( $\theta = 95.64^\circ$ )



# Effects on aperture of balloon-borne experiments

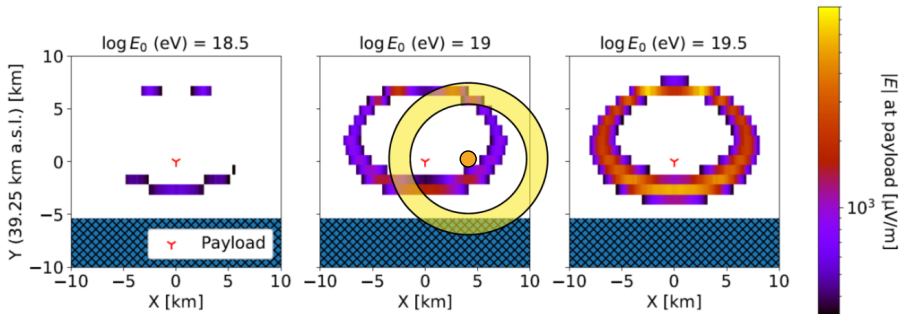
- Asymmetries in the radio emission impact the effective area of high-altitude detectors
- Example: Showers producing signals above trigger threshold of ANITA, assuming elevation angle of event 9734523 of ANITA IV ( $\theta = 95.64^\circ$ )





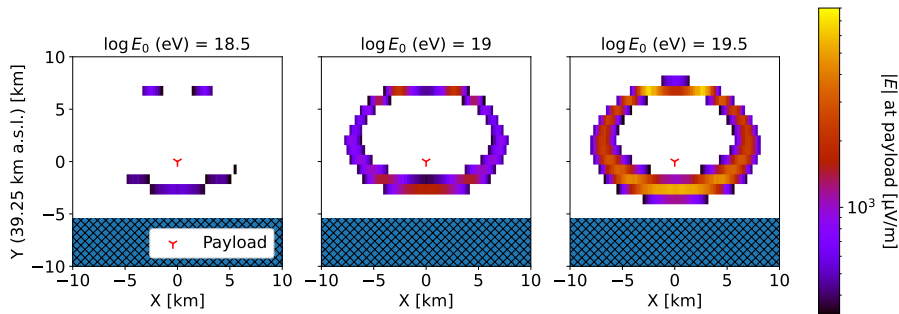
# Effects on aperture of balloon-borne experiments

- Asymmetries in the radio emission impact the effective area of high-altitude detectors
- Example: Showers producing signals above trigger threshold of ANITA, assuming elevation angle of event 9734523 of ANITA IV ( $\theta = 95.64^\circ$ )



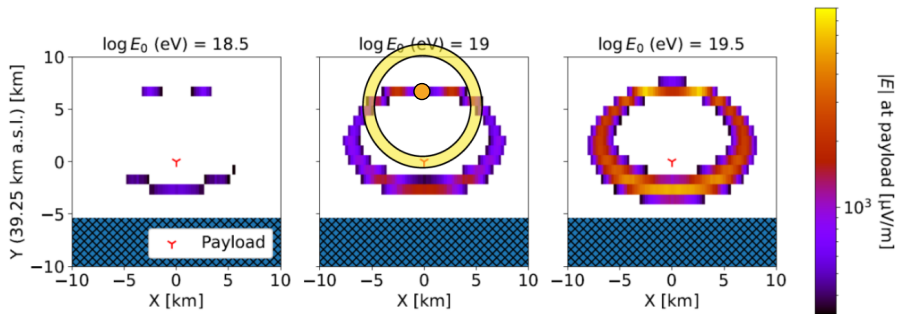
# Effects on aperture of balloon-borne experiments

- Asymmetries in the radio emission impact the effective area of high-altitude detectors
- Asymmetric effective area around the detector due to refractive effects



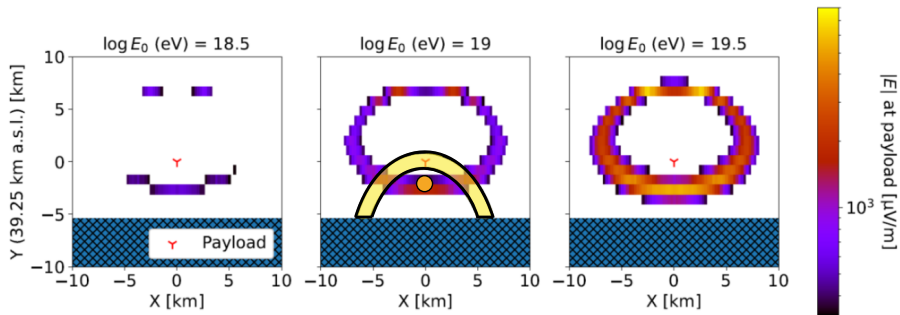
# Effects on aperture of balloon-borne experiments

- Asymmetries in the radio emission impact the effective area of high-altitude detectors
- Asymmetric effective area around the detector due to refractive effects



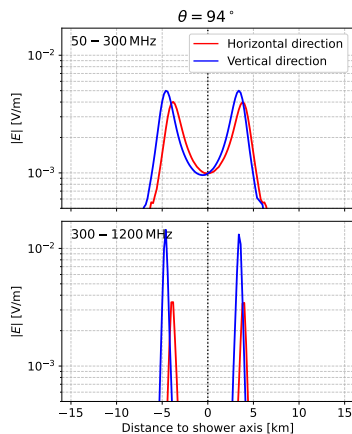
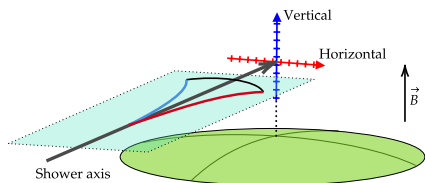
# Effects on aperture of balloon-borne experiments

- Asymmetries in the radio emission impact the effective area of high-altitude detectors
- Asymmetric effective area around the detector due to refractive effects



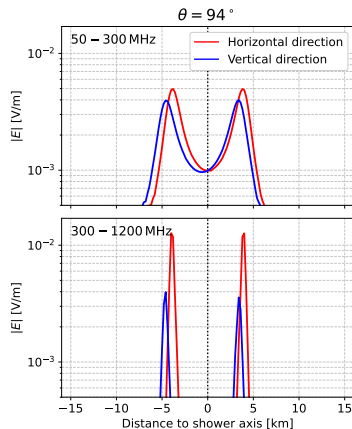
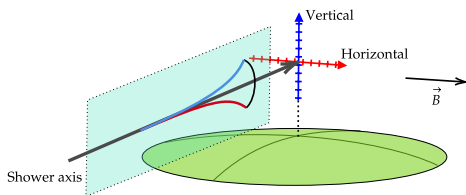
# Lateral distribution of the signal

- Geometry and dimensions of cascades affect their radio emission
- Stronger electric fields outside the  $\mathbf{v} \times \mathbf{B}$  plane: *Coherence* asymmetry
- Dependence on shower geometry, orientation w.r.t magnetic field and frequency of observation.



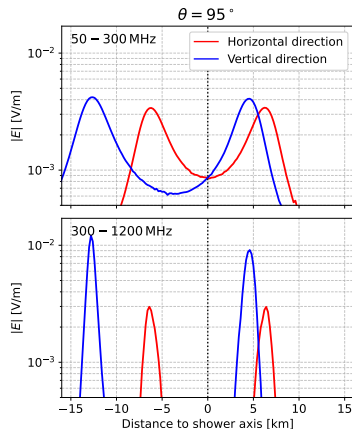
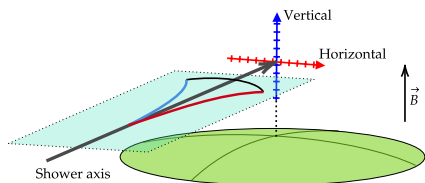
# Lateral distribution of the signal

- Geometry and dimensions of cascades affect their radio emission
- Stronger electric fields outside the  $\mathbf{v} \times \mathbf{B}$  plane: *Coherence* asymmetry
- Dependence on shower geometry, orientation w.r.t magnetic field and frequency of observation.



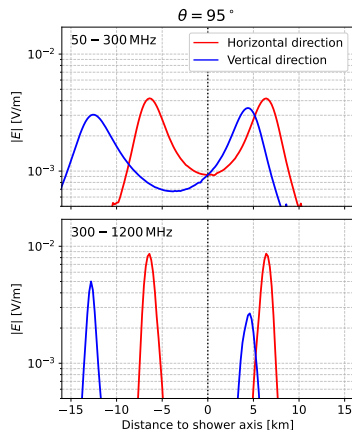
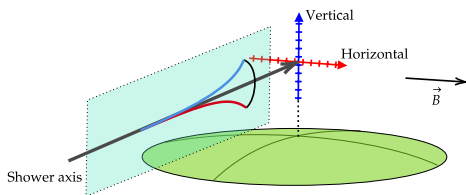
# Lateral distribution of the signal

- Geometry and dimensions of cascades affect their radio emission
- Stronger electric fields outside the  $\mathbf{v} \times \mathbf{B}$  plane: *Coherence* asymmetry
- Dependence on shower geometry, orientation w.r.t magnetic field and frequency of observation.



# Lateral distribution of the signal

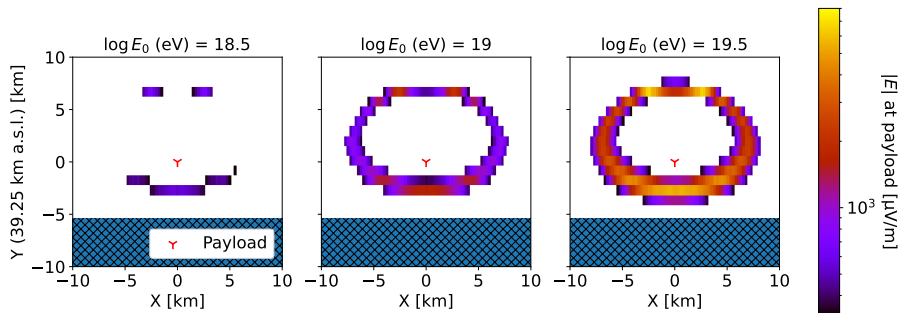
- Geometry and dimensions of cascades affect their radio emission
- Stronger electric fields outside the  $\mathbf{v} \times \mathbf{B}$  plane: *Coherence* asymmetry
- Dependence on shower geometry, orientation w.r.t magnetic field and frequency of observation.





# Effects on aperture of balloon-borne experiments

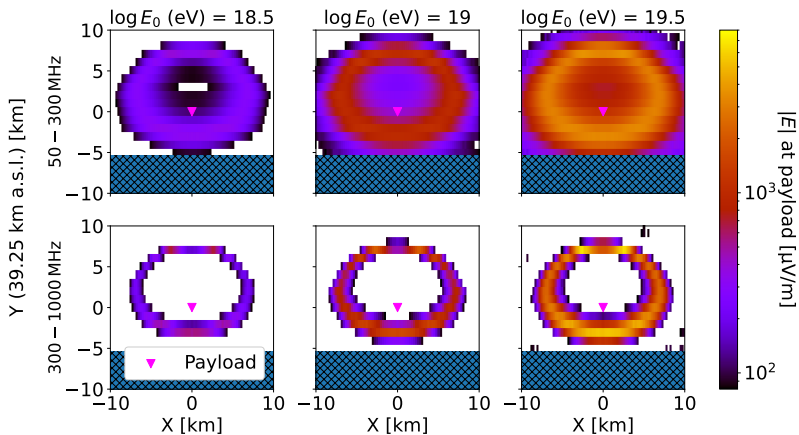
- Asymmetries in the radio emission impact the effective area of high-altitude detectors
- Coherence asymmetry: Showers leaving the detector outside their *flattening* plane ( $\mathbf{v} \times \mathbf{B}$ ) produce stronger signals (ID 9734523,  $\theta = 95.64^\circ$ )





# Future detectors

- Lower trigger thresholds will increase the number of observed events
- Instruments working in lower frequency bands will be less affected by coherence asymmetry



- 1 Introduction & Motivation
- 2 Air shower development
- 3 Characteristics of the radio emission
- 4 Conclusion & Outlook

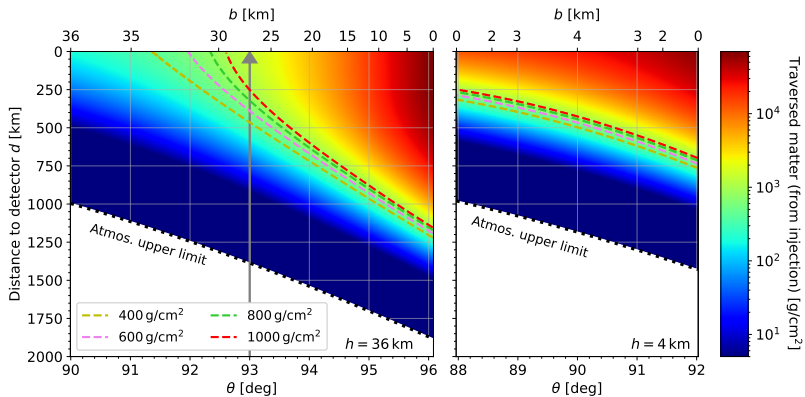
# Conclusion & Outlook

- Atmosphere-skimming air showers develop across very low densities under the effect of the geomagnetic field.
- Length scales reaching hundreds of km, strongly flattened along the  $\mathbf{v} \times \mathbf{B}$  direction
- Two distinct features in the radio emission: refractive and coherence asymmetries
- Complex dependence between shower geometry and detector position

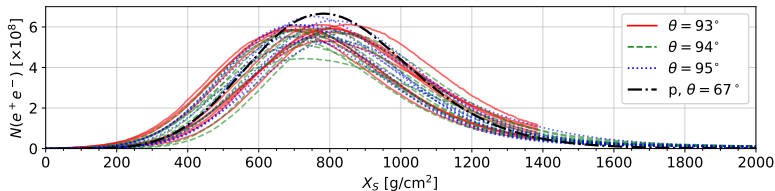
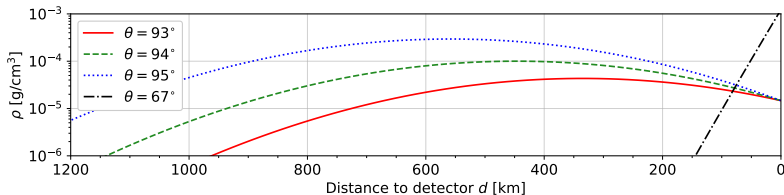
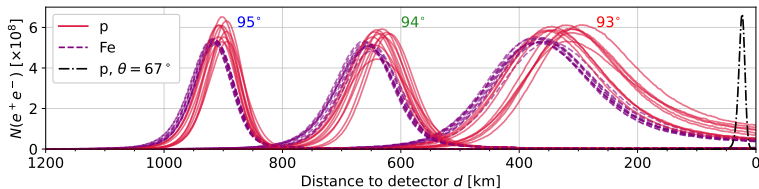
# Conclusion & Outlook

- Atmosphere-skimming air showers develop across very low densities under the effect of the geomagnetic field.
- Length scales reaching hundreds of km, strongly flattened along the  $\mathbf{v} \times \mathbf{B}$  direction
- Two distinct features in the radio emission: refractive and coherence asymmetries
- Complex dependence between shower geometry and detector position
- Detailed simulations will be needed to study how these effects influence the interpretation of collected data
- ZHAireS-RASPASS available upon request

# Backup: Phase space

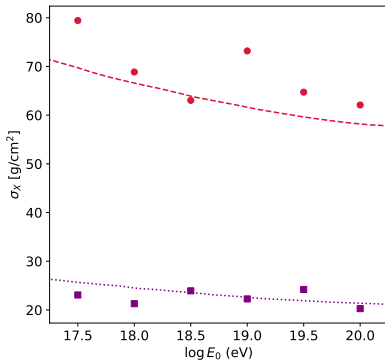
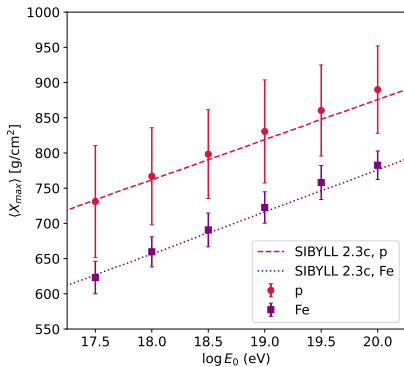


# Backup: Longitudinal development

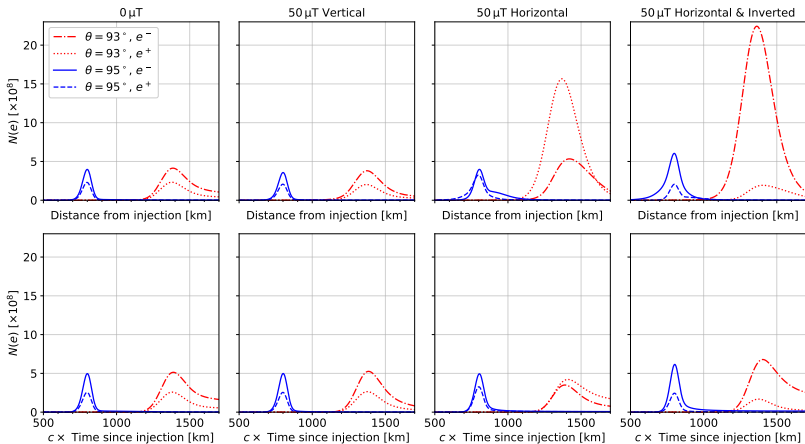




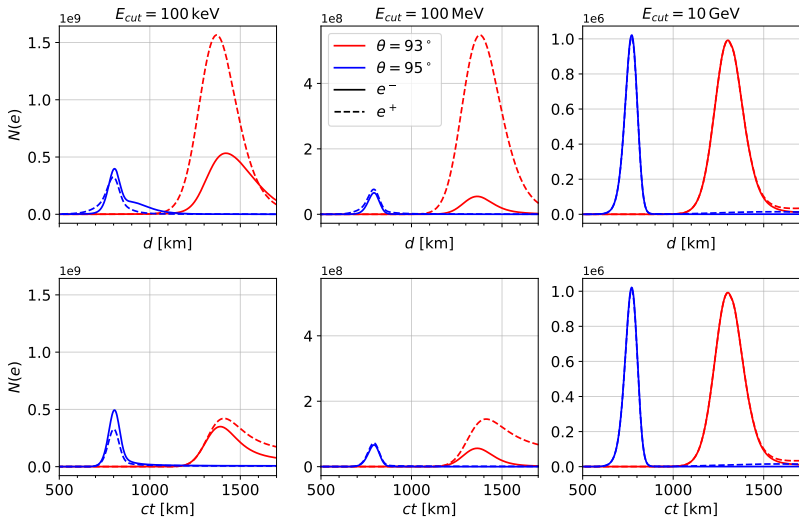
# Backup: Elongation Rate



# Backup: Longitudinal development & magnetic field effects

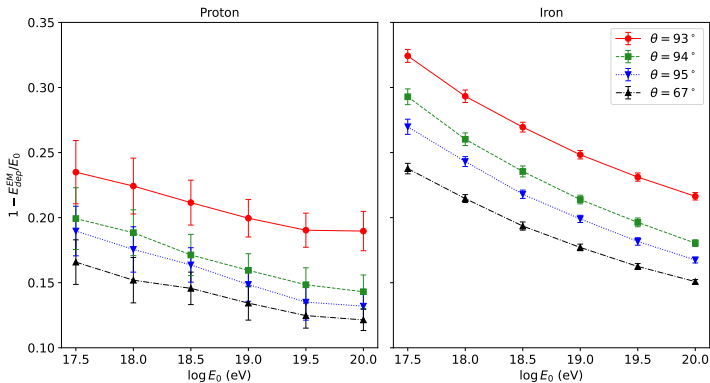


# Backup: Longitudinal development & magnetic field effects



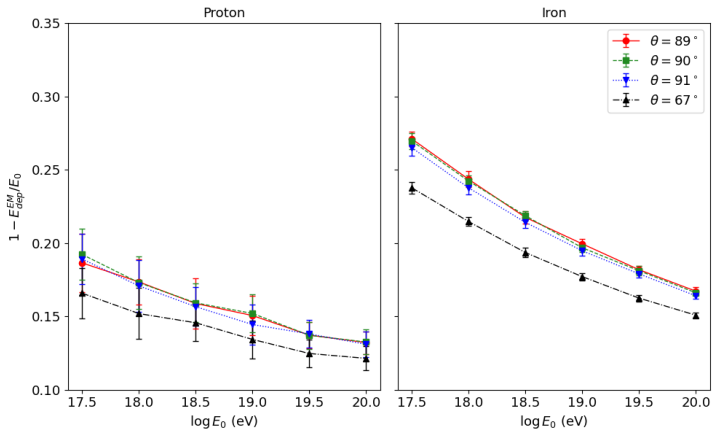
# Backup: Invisible energy for radio

- Showers passing at  $h = 36$  km



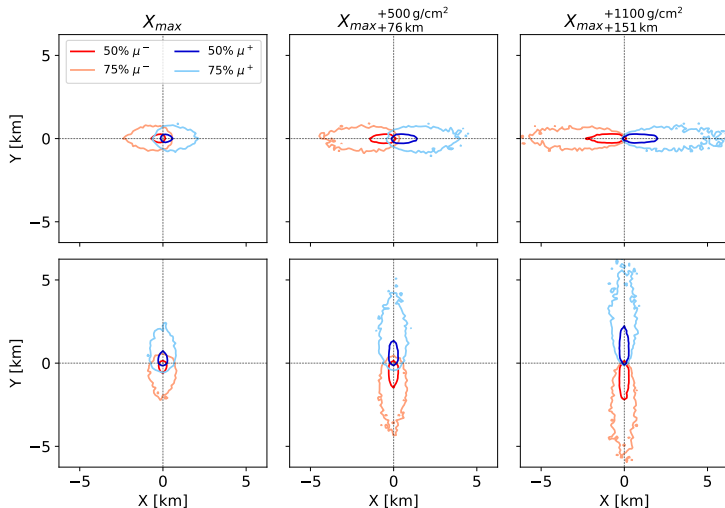
# Backup: Invisible energy for radio

- Showers passing at  $h = 4$  km



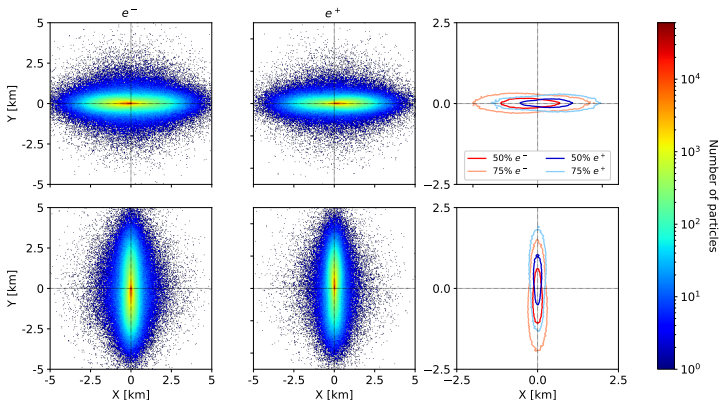
# Backup: Muon lateral development

- Proton shower with  $\theta = 94^\circ$ ,  $h = 36$  km



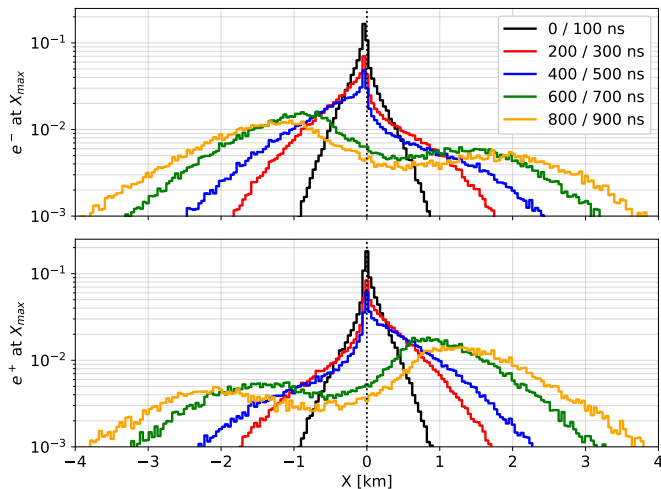
# Backup: Electron lateral development

- Proton shower with  $\theta = 94^\circ$ ,  $h = 36$  km at  $X_{\max}$



# Backup: Electron lateral development

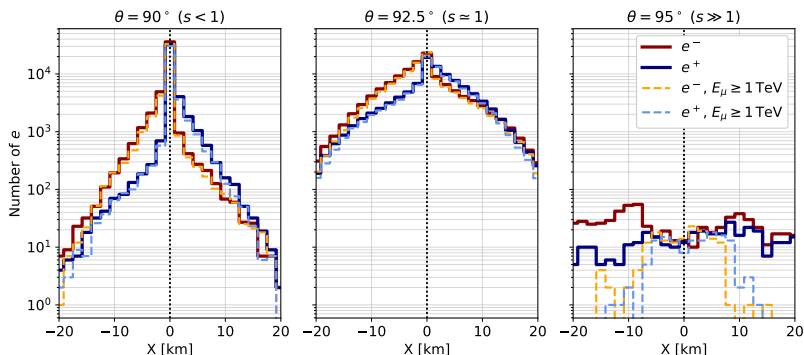
- Proton shower with  $\theta = 94^\circ$ ,  $h = 36$  km at  $X_{\max}$



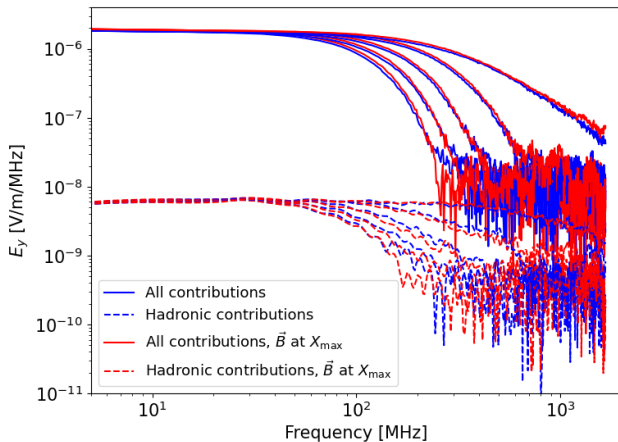


# Backup: Distribution of particles at the detector

- Proton showers with  $h = 36$  km intercepted at different ages



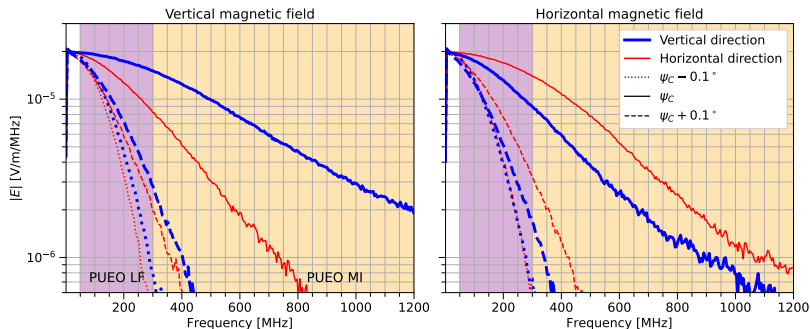
# Backup: Hadronic contribution & Constant $\vec{B}$ approx.





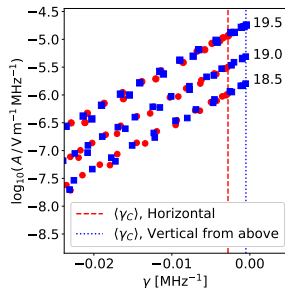
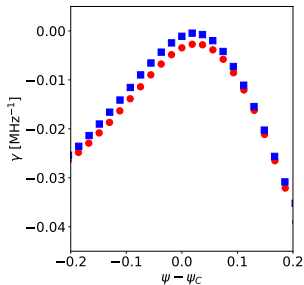
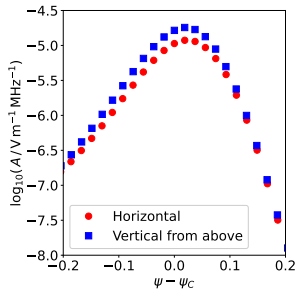
# Simulated spectra

- Reduction of high frequency content at positions inside the *flattening* plane of the shower
- Different spectral slope at equivalent off-axis positions.
- Most important differences appear close to the Cherenkov angle
- Possible effects on analysis methods based on spectral shape.



# Backup: Impact of asymmetries on spectral slopes

- Exponential fits to the spectrum in the 100 – 250 MHz band for a proton shower with  $\theta = 94^\circ$  and  $h = 36$  km



# Backup: Effective area of ANITA IV

- Assuming elevation angles for the two events detected by ANITA IV
- Multiplied by the cosmic ray flux as measured by Auger

